Quantum Electronics **51** (2) 184–188 (2021)

DIFFRACTION OPTICS

https://doi.org/10.1070/QEL17455

Limiting spectral and angular characteristics of sawtooth dual-relief two-layer diffraction microstructures

G.I. Greisukh, E.G. Ezhov, O.A. Zakharov, V.A. Danilov, B.A. Usievich

Abstract. **Sawtooth two-layer microstructures with internal and external, as well as with two internal reliefs, composed of technological and commercially available optical plastics or an optical plastic and nanocomposite material are investigated. By using the corresponding model microstructures in the frameworks of the rigorous diffraction theory, the limiting spectral and angular characteristics are estimated for sawtooth two-layer dual-relief diffraction microstructures of both types.**

Keywords: *diffractive optical element, two-layer dual-relief diffraction microstructure, diffraction efficiency, scalar and rigorous diffraction theories.*

1. Introduction

The dependence of the diffraction efficiency (DE) of diffractive optical elements (DOEs) on a radiation wavelength and angle of incidence onto the element along with technological difficulties of suppressing this dependence still prevent a wide practical employment of DOEs in image optical systems. First of all, objectives of photo and video cameras in mobile devices and mass-production security video devices are implied. In such objectives intended for operation with polychromatic radiation, the employment of DOEs seems the most promising. In this case, a high degree of correcting chromatic aberrations can be reached, which is necessary for obtaining a high-quality colour image even with a limited set of optical materials used for fabricating refractive surfaces by precision stamping [1–4].

Known effective solutions for weakening the dependence of the DE for a sawtooth relief-phase microstructure on the radiation wavelength and the angle of light incidence to the element imply the transfer from single-layer sawtooth microstructures to structures comprising several layers and reliefs [5–15] as shown in Figs 1–3.

While developing an optical system with DOEs, one should take into account both technological limitations of microstructure fabrication and potential possibilities of such microstructures to suppress the DE dependences on a radiation wavelength and angle of incidence onto the element. For double-layer single-relief microstructures, these problems are thoroughly studied and described in [16, 17], whereas in similar investigations concerning dual-relief microstructures, only first steps are taken (see, for example, [11, 17]). Results given in the present work are aimed at bridging this gap with a particular attention being paid to estimating the limiting spectral and angular characteristics of two-layer microstructures with two internal reliefs (Fig. 3 at $n' = 1$). This interest is explained by that, presently, such a microstructure is the most technological one. Indeed, it can be easily realised in the form of two close coaxial single-layer kinoform elements separated by an air gap. A commercial technology for producing and replicating such elements is well developed (see, for example, [18]). Recall that a DOE of this design was used in the first commercially produced telescopic objective [19, 20].

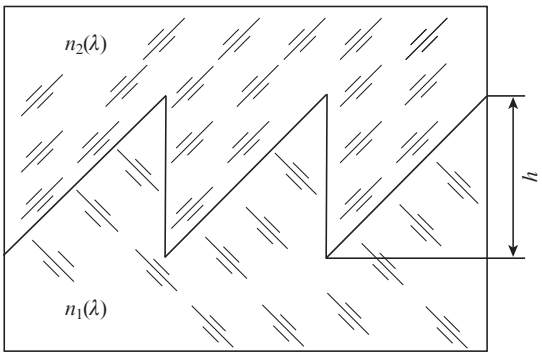

Figure 1. Two-layer single-relief sawtooth microstructure.

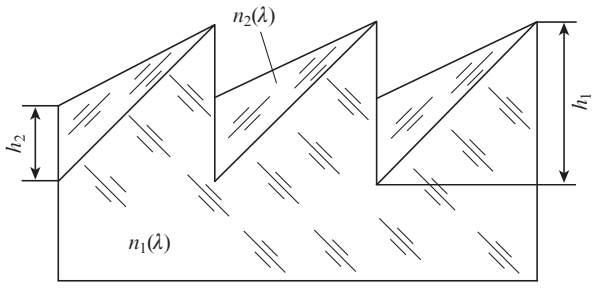

Figure 2. Two-layer sawtooth microstructure with internal and external reliefs.

G.I. Greisukh, E.G. Ezhov, O.A. Zakharov Penza State University of Architecture and Construction, ul. Germana Titova 28, 440028 Penza, Russia; e-mail: grey@pguas.ru;
V.A. Danilov Scientific and Technological Centre of Unique Instrumentation, Russian Academy of Sciences, ul. Butlerova 15, 117342 Moscow, Russia;
B.A. Usievich Prokhorov General Physics Institute of the Russian Academy of Sciences, ul. Vavilova 38, 119991 Moscow, Russia

Received 30 September 2020
Kvantovaya Elektronika **51** (2) 184–188 (2021)
Translated by N.A. Raspopov

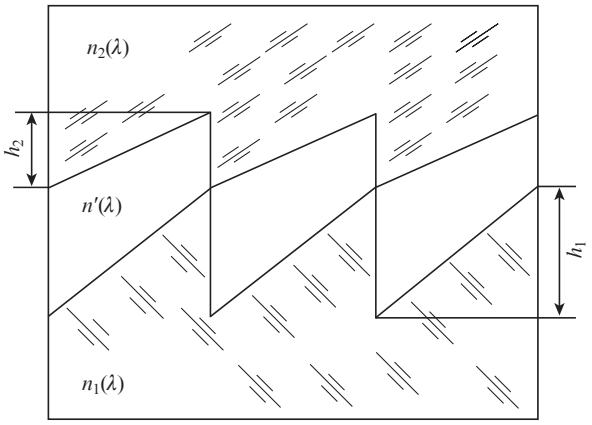

Figure 3. Three-layer dual-relief sawtooth microstructure.

2. Estimation parameters for microstructure comparative analysis

In the present work, we estimate spectral and angular characteristics of sawtooth relief–phase diffractive microstructures of various kinds by using the same parameters as in papers [16, 17]. Thus, the suppression of the DE dependence on the wavelength at normal radiation incidence to a microstructure is estimated by using the local and integral Q-factors of a microstructure, calculated in the framework of the scalar diffraction theory (SDT). A local Q-factor is equal to the maximal absolute value of the parameter

$$Q_i = \frac{\Delta l(\lambda_i)}{\lambda_i} - 1, \tag{1}$$

that is, $Q_{\text{loc}} = |Q_i|_{\max}$. Here $\Delta l(\lambda_i)$ is the optical path increment per one period of the microstructure.

In the case of two-layer microstructures with two internal (Fig. 3 at $n' = 1$) or one internal and one external reliefs (Fig. 2), the optical path increment is given by the expression [9]

$$\Delta l(\lambda_i) = h_1[n_1(\lambda_i) - 1] - h_2[n_2(\lambda_i) - 1]. \tag{2}$$

It worth noting that from the viewpoint of SDT, the microstructures shown in Fig. 2 and Fig. 3 at $n' = 1$ are absolutely similar, whereas in the rigorous diffraction theory they differ in the relief effective depth h_{eff}. The microstructures in Figs 2 and 3 have $h_{\text{eff}} = h_1$ and $h_{\text{eff}} = h_1 + h_2$, respectively.

The absolute value of Q_i (1) determines how much the DE calculated in the framework of SDT at a wavelength λ_i reduces due to the nonlinear dependence $\Delta l(\lambda_i)$ in the operation spectral range ($\lambda_{\min} \leqslant \lambda \leqslant \lambda_{\max}$). The integral Q-factor of a microstructure takes into account a negative consequence of the nonlinearity $\Delta l(\lambda_i)$ in the whole operation spectral range:

$$Q_{\text{int}} = \sqrt{\frac{1}{i_{\max}} \sum_{1}^{i_{\max}} Q_i^2}. \tag{3}$$

Note that Q-factors can only promptly juxtapose optical material combinations for a multilayer sawtooth microstructure and make it possible to choose the most promising combinations from the viewpoint of suppressing the DE dependence on a wavelength. A reliable estimate of the DE dependence on the angle of light incidence onto a microstructure can be obtained only in the framework of a rigorous diffraction theory by solving Maxwell's equations, in particular, using the so-called method of rigorous coupled-wave analysis (RCWA) [21].

Obviously, an estimation of the microstructure relief depths and maximal admissible angles of light incidence depends on a choice of the appropriate criterion. If light diffraction to side diffraction orders is undesirable at all wavelengths from the operation spectral range, then the criterion suggested in [12] is the most adequate. According to this criterion, the relief depths are optimal if in the chosen spectral range the maximal possible range is provided for light incidence angles ψ within which the DE (at the point of its minimum) is at least the minimal admissible value, which is 0.95 of the DE maximal value under normal incidence onto a microstructure substrate [$\eta^{(\psi)}_{\text{EM min}} / \eta^{(\psi=0)}_{\text{EM max}} \geqslant 0.95$)]. This value guarantees that not only halo is absent, but also any observable negative influence of side diffraction orders on a quality of the image formed by an optical system with DOE. This criterion has been successfully used in a number of papers (see, for example, [13–15]).

Importantly, the absolute value of the negative angle of light incidence onto a structure $|\psi_-|$ and the value of positive angle of incidence ψ_+, at which the DEs estimated by the RCWA method falls to equal levels, may, however, substantially differ. Therefore, similarly to [11–15], for the estimated (the maximal admissible) angle Ψ in the present work we take the smallest from the angles $|\psi_-|$ and ψ_+. Further as in the SDT calculations we assume, that the radiation passes from air to a microstructure from the side of the material possessing the refractive index $n_1(\lambda)$, and the angle Ψ is counted from the normal to the substrate.

If the relief depths and combination of the optical materials chosen for a sawtooth microstructure ensure that both the Q-factors are zero ($Q_{\text{loc}} = Q_{\text{int}} = 0$), then the DE calculated by the RCWA method at normal light incidence $\eta^{(\psi=0)}_{\text{EM}}$ will be close to unity. In this case, Fresnel losses will mainly contribute into the DE reduction at all wavelengths from the operation spectral range. The maximal admissible angle of light incidence [that is, the estimation angle Ψ, corresponding to the condition $\eta^{(\psi)}_{\text{EM min}} / \eta^{(\psi=0)}_{\text{EM max}} \geqslant 0.95$)] at the optimal relief depths will depend on the microstructure type, effective relief depth, and relative spatial period $P = \Lambda / h_{\text{eff}}$.

3. Results of the comparative analysis of two-layer sawtooth microstructures

Table 1 presents the data on the two-layer dual-relief sawtooth microstructures composed of a number of pairs of optical materials intended for operation in the visible spectral range ($0.4 \leqslant \lambda \leqslant 0.7$ μm), for which the DE spectral and angular dependences have been maximally suppressed.

In the last column of Table 1, there are references to the papers, in which results of first investigations are discussed pertaining to a microstructure composed from the corresponding pair of optical materials. Note that the optimal relief depths and maximal admissible angles of light incidence onto a microstructure may not coincide with data from the paper in which this microstructure has been studied for the first time. This is explained by that all the parameters mentioned have been recalculated according to the goals of the present work. For technological and commercially available plastics PMMA, POLYCARB (PC), POLYSTYR (PS), and E48R, we used dispersion formulae from catalogues Mics and

Table 1. Parameters and angular characteristics for a number of two-layer dual-relief microstructures.

Microstructure number	Microstructure type	Optical materials of two layers with the reflective indices n_1/n_2	Q_{loc}	Q_{int}	h_1/μm	h_2^{opt}/μm	Ψ/deg	References
1	Fig.2	PMMA/PC	0.1283	0.058	15.1	11.67 11.70 11.70	9.5 at $P = 10$ 15.0 at $P = 20$ 16.8 at $P = 30$	[9]
	Fig.3	PMMA/PC	0.1283	0.058	15.1	11.68 11.67 11.67	7.2 at $P = 10$ 7.5 at $P = 20$ 10.5 at $P = 30$	[11]
2	Fig.2	PMMA/mathematical model	0	0	15.1	11.745 11.75 11.75	16 at $P = 10$ 19.5 at $P = 20$ 21.0 at $P = 30$	[17]
	Fig.3	PMMA/mathematical model	0	0	15.1	11.75 11.77 11.77	13.4 at $P = 10$ 18 at $P = 20$ 20.5 at $P = 30$	this paper
3	Fig.2	E48R/PS	0.1193	0.054	16.3	13.665 13.69 13.69	10.7 at $P = 10$ 15.5 at $P = 20$ 19.4 at $P = 30$	this paper
	Fig.3	E48R/PS	0.1193	0.054	16.3	13.65 13.68 13.68	7.3 at $P = 10$ 12.5 at $P = 20$ 14.5 at $P = 30$	this paper
4	Fig.2	E48R/mathematical model	0	0		13.72 13.745 13.745	15.4 at $P = 10$ 22.5 at $P = 20$ 23 at $P = 30$	this paper
	Fig.3	E48R/mathematical model	0	0		13.73 13.745 13.745	11.5 at $P = 10$ 19 at $P = 20$ 20.6 at $P = 30$	this paper
5	Fig.2	E48R/ITO in PMMA	0.0520	0.025		3.26 3.26 3.26	16.7 at $P = 10$ 23.5 at $P = 20$ 25 at $P = 30$	this paper
	Fig.3	E48R/ITO in PMMA	0.0520	0.025	4.72	3.26 3.26 3.26	14.5 at $P = 10$ 18.5 at $P = 20$ 22.3 at $P = 30$	this paper
6	Fig.2	E48R(ITO)/ mathematical model	0	0	4.72	3.235 3.26 3.26	18.5 at $P = 10$ 25.5 at $P = 20$ 26 at $P = 30$	this paper
	Fig.3	E48R(ITO)/ mathematical model	0	0	4.72	3.255 3.27 3.27	14.5 at $P = 10$ 21.3 at $P = 20$ 22.8 at $P = 30$	this paper

Zeon of Glasscat database from Zemax optical designing program [22]. As for the nanocomposite material ITO in PMMA, which was used for assembling microstructure 5, the dependence of its refractive index on wavelength is described by the Sellmeyer formula:

$$n^2 - 1 = \frac{K_1\lambda^2}{\lambda^2 - L_1} + \frac{K_2\lambda^2}{\lambda^2 - L_2} + \frac{K_3\lambda^2}{\lambda^2 - L_3}. \quad (4)$$

The values of coefficients K_{1-3} and L_{1-3} kindly presented by authors of paper [23] are as follows: $K_1 = 1.21406$, $K_2 = 0.48463$, $K_3 = 2.98136$, $L_1 = 0.00489$, $L_2 = 0.04373$, and $L_3 = 5.19483$.

The relief depthsв h_1 and h_2, at which the value of parameter Q_{loc} is minimal within the visible spectral range (0.4 μm $\leqslant \lambda \leqslant$ 0.7 μm), were obtained for microstructures 1, 3, and 5 by the method described in [17]. Then, the optimal relief depths h_2^{opt} and the intervals for incident angles, within which the inequality $\eta_{EM\,min}^{(\psi)}/\eta_{EM\,max}^{(\psi=0)} \geqslant 0.95$ holds, were found by the RCWA method using the MC Grating program [24] at a relief depth h_1 and two values of relative period $P = 10$ and 20. Finally, for each microstructure, the corresponding angle intervals were calculated at $P = 30$ from the depths h_1 and h_2^{opt} found at $P = 20$. For each angle interval obtained, the interval boundary with the lowest modulus is included in Table 1 as the maximal admissible angle Ψ.

Potential possibilities of studied microstructures were analysed by using the model microstructures 2, 4, and 6 suggested in [16, 17]. In the process of composing the optical materials with the refractive indices $n_1(\lambda)$ were the same as in parent microstructures 1, 3, and 5; materials of the second layers were replaced by the corresponding mathematical model that provided the fulfilment of the condition $Q_{loc} = Q_{int} = 0$. The refractive indices of the model materials were calculated by the formula

$$n_2(\lambda_i) = \frac{h_1}{h_2}[n_1(\lambda_i) - 1] - \frac{\lambda_i}{h_2} + 1. \quad (5)$$

Here, the relief depths h_1 and h_2 were taken equal to those of parent structures; however, at the stage of RCWA calculation the relief depth h_2 was optimised similarly to parent microstructures.

The data given in Table 1 lead us to make the following conclusions:

1. Only two pairs of technological and commercially available optical plastics give a possibility to compose two-layer dual-relief sawtooth microstructures with a relief depth

$h_1 < 20$ μm and the DE dependence on a wavelength in the visible spectral range, reduced to an admissible level. These microstructures (1 and 3) are characterised by rather close values of the relief depths at which the Q-factors are minimal, close values of Q-factors themselves and, as a sequence, maximal admissible light incident angles.

2. If a nanocomposite material is used in two-layer dual-relief microstructures along with a commercially available optical plastic material, then the relief depth h_1 providing minimal Q-factors reduces more than thrice, and the values of the Q-factors fall by a factor of two and more.

3. The maximal admissible angle of light incidence Ψ increases with increasing relative spatial period P for all the microstructures.

4. When microstructures are composed of the same pair of optical materials, and have equal values P, the angle Ψ is always greater for the microstructure having the internal and external reliefs such that $h_{\text{eff}} = h_1$ (Fig. 2) as compared to the microstructures with two internal reliefs such that $h_{\text{eff}} = h_1 + h_2$ (Fig. 3). In the studied interval of parameter P values ($10 \leqslant P \leqslant 30$), the angle Ψ for the microstructures with deep reliefs ($h_1 > 15$ μm) composed according to Fig. 2 is, on the average, 1.5 times greater than for microstructures composed as in Fig. 3. For the microstructure with $h_1 \approx 4.7$ μm, the angle Ψ is greater by a factor of 1.2.

5. The maximal admissible angles of light incidence onto model microstructures 2 and 4 can be considered as the limiting angles for two-layer dual-relief microstructures with deep reliefs ($h_1 > 15$ μm). In this case, a comparison of microstructures 1 and 3 with microstructures 2 and 4 shows that the maximal admissible angles for the microstructures composed of real materials according to Fig. 2 are less than the limiting angles for microstructures of this type by a factor of 1.2–1.7 depending on the parameter P. The maximal admissible angles for microstructures composed of real materials according to Fig. 3 are less than the limiting angles by a factor of 1.42–2.4 depending on the parameter P.

6. Microstructure 5 composed of a nanocomposite material according to Fig. 2 has the maximal admissible angle of light incidence, which at $P = 10$ exceeds the corresponding angle of microstructures based on commercially available plastics by a factor of approximately 1.6, and at $P = 30$ the excess factor is about 1.4. In the case of forming a microstructure with two internal reliefs (Fig. 3), the maximal admissible angle of light incidence at $P = 10$ exceeds the corresponding angle of microstructures based on commercially available plastics by a factor of approximately 2; at $P = 30$ this factor is about 1.8. Moreover, a comparison of microstructures 5 and 6 shows that the maximal admissible angles of light incidence onto the microstructure composed of real materials and onto a model microstructure actually coincide.

7. In view of the above discussion and taking into account the fact that from known optical materials (suitable for fabricating DOEs) the minimal possible relief depth is provided by microstructures 5, the maximal admissible angles of radiation incidence onto microstructures 5 and 6 can be considered as the limiting values for two-layer dual-relief sawtooth microstructures.

4. Conclusions

By using the local and integral Q-factors calculated in the framework of SDT for a two-layer dual-relief sawtooth microstructure, the pairs of optical plastics are chosen, which suppress the DE dependences on the wavelength in the visible spectral range at the greatest relief depth of at most 16.3 μm. There are two such pairs: PMMA/PC and E48R/PS. In microstructures composed of these pairs, the Q-factors are close to zero, and DE at normal incidence is close to unity over the whole visible spectral range. Microstructures with internal and external (Fig. 2) reliefs are indistinguishable from those with two internal reliefs (Fig. 3), because in the scalar approximation the both are calculated by the same formulae.

In the framework of the rigorous theory, an analysis of the two compositions differing in the relief depths ($h_{\text{eff}} = h_1$ for the microstructure with an internal and external reliefs, and $h_{\text{eff}} = h_1 + h_2$ for the microstructure with two internal reliefs) yields different DE values especially at inclined incidence of light. Such an analysis performed by the RCWA method shows that admissible angles of light incidence onto a microstructure depend both on the effective relief depth, and on its relative spatial period $P = \Lambda/h_{\text{eff}}$. In the case of equal values P, microstructures with internal and external reliefs have a greater angle Ψ than microstructures with two internal reliefs. In the investigated range of P values ($10 \leqslant P \leqslant 30$), the microstructures with deep reliefs ($h_1 > 15$ μm) composed according to Fig. 2 have, in average, an angle Ψ greater by a factor of 1.5 than microstructures composed according to Fig. 3. For microstructures with $h_1 \approx 4.7$ μm, angle Ψ is 1.2 times greater.

The limiting angles of light incidence onto two-layer dual-relief microstructures with deep reliefs ($h_1 > 15$ μm) estimated from the corresponding angles for model microstructures are (depending on the composition scheme and parameter P) 1.2–2.4 times greater than the maximal admissible angles of light incidence onto the microstructures composed of real materials. At $10 \leqslant P \leqslant 30$, the limiting angles are in the range of 15° – 23° for the composition with internal and external reliefs and in the range of 11.5°–20.6° for the composition with two internal reliefs.

The employment of a nanocomposite material (ITO in PMMA) presented in [23, 25] for the assembly of two-layer dual-relief microstructures together with a commercially available optical plastic E48R makes it possible to reduce more than thrice the greater depth (from the two relief depths) at which the Q-factors are minimal, and reduce more than twice the values of the Q-factors themselves. Such a reduction is accompanied by an increase in the maximal admissible incident angles. The angles for the microstructure composed of real materials actually coincide with the corresponding incident angles for the model microstructure.

From the optical materials suitable for producing DOE, E48R and ITO in PMMA provide the minimal possible relief depths. Thus, for today the maximal admissible angles of light incidence onto a structure composed of such materials can be considered as the limiting angles for two-layer dual-relief sawtooth microstructures. At $10 \leqslant P \leqslant 30$, these angles are within the range of 16.7°–25° for the composition with internal and external reliefs and in the range of 14.5°–22.3° for the composition with two internal reliefs.

A comparison of the limiting incident angles for two-layer dual-relief sawtooth microstructures with those for the two-layer single-relief microstructures discussed in [16, 17] shows that the limiting angles for two-relief sawtooth microstructures composed of technological and presently commercially available optical plastics are insignificantly inferior to the corresponding angles of single-relief microstructures that comprise a pair of optical materials including plastic and a special

precision stamped glass. However, when nanocomposite materials are used for composing two-layer microstructures, the limiting angles of light incidence onto single-relief microstructures are more than twice greater than those for two-relief microstructures.

Acknowledgements. The authors are grateful to the authors of paper [23] for the possibility of using the dispersion formulae for their nanocomposite materials.

The work was supported by the Russian Science Foundation (Project No. 20-19-00081).

References

1. Hua H. et al. *Appl. Opt*., **42**, 97 (2003).
2. Greisukh G.I. et al. *Appl. Opt*., **49**, 4379 (2010).
3. Greisukh G.I. et al. *Appl. Opt*., **52**, 5843 (2013).
4. Antonov A.I. et al. *Optoelectron. Instrum. Data Proces.*, **53**, 4 (2017) [*Avtometriya*, **53**, 4 (2017)].
5. Lukin A.V. Patent of the Russian Federation No. 1271240 (1985).
6. Lukin A.V. *J. Opt. Technol*., **74**, 65 (2007) [*Opt. Zh*., **74**, 80 (2007)].
7. Ebstein S.T. *Proc. SPIE*, **2404**, 211 (1995).
8. http://www.jeos.org/index.php/jeos_rp/article/view/176.
9. Greisukh G.I. et al. *Opt. Spectrosc*., **106**, 621 (2009) [*Opt. Spektrosk*., **106**, 621 (2009)].
10. Greisukh G.I. et al. *Opt. Commun*., **338**, 54 (2015).
11. Greisukh G.I. et al. *Opt. Spectrosc.*, **118**, 964 (2015) [*Opt. Spektrosk*., **118**, 997 (2015)].
12. Greisukh G.I. et al. *J. Opt. Technol*., **82**, 308 (2015) [*Opt. Zh*., **82**, 56 (2015)].
13. Greisukh G.I. et al. *Opt. Spectrosc*., **124**, 98 (2018) [*Opt. Spektrosk*., **124**, 100 (2018)].
14. Greisukh G.I. et al. *Opt. Spectrosc*., **125**, 232 (2018) [*Opt. Spektrosk*., **125**, 57 (2018)].
15. Greisukh G.I. et al. *Computer Optics*, **42**, 38 (2018) [*Komp'yuternaya Opt*., **42**, 38 (2018)].
16. Greisukh G.I. et al. *J. Opt.*, **22**, 085604 (2020).
17. Greisukh G.I. et al. *Quantum Electron*., **50**, 623 (2020) [*Kvantovaya Elektron*., **50**, 623 (2020)].
18. https://www.edmundoptics.com/f/plastic-hybrid-aspheric-lenses/13921/.
19. https://doi.org/10.1364/DOMO.2002.DMA2.
20. http://www.shopfoto.ru/p/canon-ef-400-mm-f4-do-is-usm.
21. Moharam M.G. et al. *J. Opt. Soc. Am*., **72**, 1385 (1982).
22. http://www.radiantzemax.com.
23. Werdehausen D. et al. *Optica*, **6**, 1031 (2019).
24. http://www.mcgrating.com.
25. Werdehausen D. et al. *J. Opt.*, **22**, 065607 (2020).